Central European Journal of Energetic Materials
ISSN 1733-7178; e-ISSN 2353-1843

Cent. Eur. J. Energ. Mater. 2025, *22*(1): 46-74; DOI 10.22211/cejem/203299
Supporting Information is available in PDF-format, in colour, at:
https://ipo.lukasiewicz.gov.pl/wydawnictwa/cejem-woluminy/vol-22-nr-1/

Research paper

Suppression by Water Mist in HMX Explosions

Yang Liu[1)], **Yu Qiu**[1)], **Huinan Wang**[2)], **Keqin Zhang**[3)], **Bowen Du**[4)], **Yuewen Lu**[4)], **Jianren Zhang**[3)], **Lei Sun**[4)], **Zhixing Lv**[4,*)], **Lishuang Hu**[1,**)]

[1)] *School of Environment and Safety Engineering, North University of China, Taiyuan 030051, China*

[2)] *Shanxi North Xing'an Chemical Industry Co., Ltd., Taiyuan 030008, China*

[3)] *Shanxi Jiangyang Chemical Co., Ltd., Taiyuan 030041, China*

[4)] *Explosive Engineering and Safety Technology Research Institute of Ordnance Industry, Beijing 100053, China*

* *E-mails:* *) lvzhixing0924@163.com; **) hlsly1314@163.com

Abstract: The inhibitory effect of water mist on suspended HMX explosions and stacked HMX combustions was investigated. The impact of water mist on HMX explosions was assessed by analyzing variations in flame propagation, explosion pressure and temperature, while its effect on HMX combustions was evaluated by examining changes in the flame extinguishing time. The results reveal that both the explosion pressure and temperature of suspended HMX increase with an increase in mass. Water mist significantly influences the suppression of HMX explosions. The attenuation of explosion pressure and temperature caused by water mist in HMX explosions increases with higher spray pressures. At a spray pressure of 4.0 MPa, the explosion pressure of suspended HMX was measured at only 0.2402 MPa, representing a reduction of 52.0% in peak pressure compared to the scenario without water mist, where the explosion pressure was recorded at 0.5008 MPa. The explosion temperature was recorded at 132 °C, which is 84.3% lower than the temperature of suspended HMX explosions without water mist, measured at 840 °C. The extinguishing time of stacked HMX combustion decreases with increasing spray pressure. At a spray pressure of 4.0 MPa, the extinguishing time of stacked HMX combustion was only 49.00 ms.

Keywords: explosives and propellants, dust explosion, explosion inhibition, HMX, water mist

1 Introduction

The application of water mist in fire extinguishing began in the 1940s. Early research on water mist fire suppression by Braidech [1] and Rasbash *et al.* [2] identified two primary mechanisms: cooling and the dilution of combustible gases with water vapour. Subsequently, Wighus *et al.* [3, 4] conducted experimental studies that demonstrated the effectiveness of water vaporization in diluting combustible gases. Additionally, Mawhinney *et al.* [5, 6] found that water mist can block combustion flames and attenuate flame radiation, which are also significant factors in flame extinction. While numerous studies have explored the use of water mist in oil combustion [7-9], and gas and dust explosions, there is limited research on its effectiveness in suppressing explosive detonations.

Eriksson [10] was the first to utilize water as a wave-absorbing medium for shock wave reduction in explosives storage rooms in 1974. The study demonstrated that water can mitigate peak explosion pressure and specific impulse. Keenan *et al.* [11] designed an arsenal model with a scale ratio of 1:12, which contained a TNT pellet with a charge mass of 2.12 kg. This model was placed in a sealed laboratory with a volume of 32.56 m^3, filled with water. Experiments indicated that the peak pressure and specific impulse of the explosive gas could be significantly reduced, with the peak overpressure after the explosion decreased by more than 25%. Marchand *et al.* [12] established a setup with rainwater surrounding a specified mass of TNT explosive to compare the effect of rainwater on the attenuation of explosion shock wave pressure. The experiment revealed that after the addition of rainwater, the explosion shock wave pressure of the explosive decreased from 2.46 to 1.703 MPa. Schwer *et al.* [13, 14] employed a simulation method to investigate the attenuation characteristics of TNT explosions under the influence of water mist. Their findings indicated that water mist significantly reduced shock wave pressure, with droplet size and fog flux playing crucial roles in diminishing shock wave intensity. Resnyansky *et al.* [15] conducted experiments using various nozzles to generate water mist with different parameters, evaluating its explosion mitigation effect on bare charges in air. The results demonstrated that the pressure peak at a distance of 1.5 m from the charge was reduced by more than 80% when water mist was present compared to conditions without it. Willauer *et al.* [16] reported the effect of fine water mist on the overpressure generated by the detonation of 50 lb TNT

and 50 lb TNT-equivalent Destex explosives in a chamber. In the presence of fine water mist, the impulse, initial shock wave, and quasi-static overpressure of the 50 lb TNT explosion were reduced by 40%, 36%, and 35%, respectively. For the Destex explosion, these values were reduced by 43%, 25%, and 33%, respectively. These findings indicate that fine water mist can significantly diminish the explosion overpressure of high-energy explosives. Ananth *et al.* [17] investigated the mechanism by which fine water mist attenuated shock waves from RDX explosions using simulation methods. They found that the latent heat absorption of the water mist was the primary influencing factor, followed by the heat absorption of water vapor and the momentum absorbed by sub-droplets from the high-speed gas. Jiba *et al.* [18] examined the effect of fine water mist on the explosion of 20 g of PE4 explosive in a semi-closed explosion chamber. The results indicated that the presence of fine water mist can delay the peak arrival time of shock waves, reduce peak overpressure, and shorten the optical radiation lifetime of the fireball. Zhao [19, 20] found that when the mass ratio of water to explosives is between 2 and 2.5, water can reduce the peak overpressure of the shock wave generated by a TNT explosion by approximately 40%. Chen *et al.* [21] utilized fluid dynamics simulation software to investigate the effect of varying water-wall widths and heights on the attenuation of explosive shock waves. Zhang *et al.* [22] investigated the effect of water curtains on shock wave attenuation and discovered that when the specific distance ranged from 1.71 to 3.42 $m \cdot kg^{-1/3}$, the reduction in reflected shock wave overpressure varied from 36.3% to 94.5%. Xu *et al.* [23-26] designed a closed spherical experimental apparatus to explore the influence of water on explosion shock wave overpressure. The results indicated that water plays a dual role in enhancing and attenuating explosion overpressure, depending on distance. Li [27] investigated the attenuation effect of water bags on TNT explosion shock waves and found that the water medium significantly mitigates both quasi-static air pressure and shock wave intensity. Chen [28] developed a cabin scaling model and conducted experiments on water mist explosion suppression using this model. The results demonstrated that the overpressure and quasi-static pressure generated after an explosion within the cabin are substantially reduced by the application of water mist.

There are few research reports on the suppression of explosives using water mist. Existing studies have primarily focused on passive protection, which means that the shock wave is attenuated only after it interacts with water following an explosion. Furthermore, these studies do not include the suppression of explosive dust clouds. Consequently, this article presents research on the active suppression of HMX combustion using water mist. The aim of this research is to provide foundational data for proactive protection measures in the explosives industry.

2 Experimental Materials and Equipment

2.1 Experimental materials

The HMX was obtained from Gansu Yinguang Chemical Industry Group Co., Ltd., with a median particle diameter D_{50} of 13.09 μm, as shown in Figure 1. Before conducting the experiments, the HMX was placed in a water bath oven at 60 °C for 24 h.

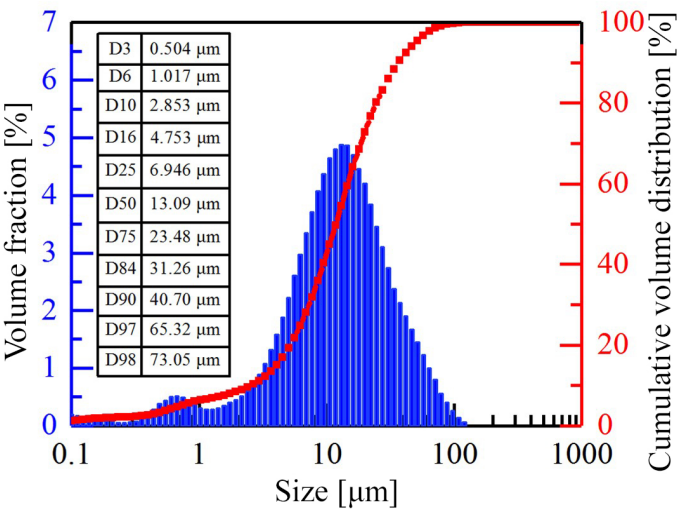

Figure 1. HMX particle size distribution

2.2 Explosion suppression of suspension HMX using water mist

The suspended HMX explosion water mist suppression tests were conducted using a self-designed visual dust explosion device, as illustrated in Figure 2. The experimental system consists of a visual square tube, a powder spraying system, an ignition system, a water mist generation system, a pressure and temperature data collection system, a high-speed camera system, and a timing control system. The pressure collection system included a pressure sensor, a pressure collection instrument, and a computer. A PCB 113B21 pressure sensor was selected and positioned 505 mm from the bottom of the square tube. The temperature acquisition system comprised a high-response thermocouple, a temperature acquisition instrument, and a computer. The thermocouple was a fast-response K-type thermocouple manufactured by LABFACILITY in the UK. It was located 370 mm from the bottom of the square tube, had a diameter of 0.5 mm, and a response time of less than 12 ms. The high-speed camera

system included a high-speed camera and a computer. The explosion flame was recorded using a high-speed camera (model: X113) from HF Agile Device Co., Ltd. The explosion inhibition device consisted of a flame detector, a controller, and a quick-opening device. The timing controller was designed based on a microcontroller and utilized an external control switch to set the timing for the 6-channel G6K-2P-Y-24 VDC Omron relays.

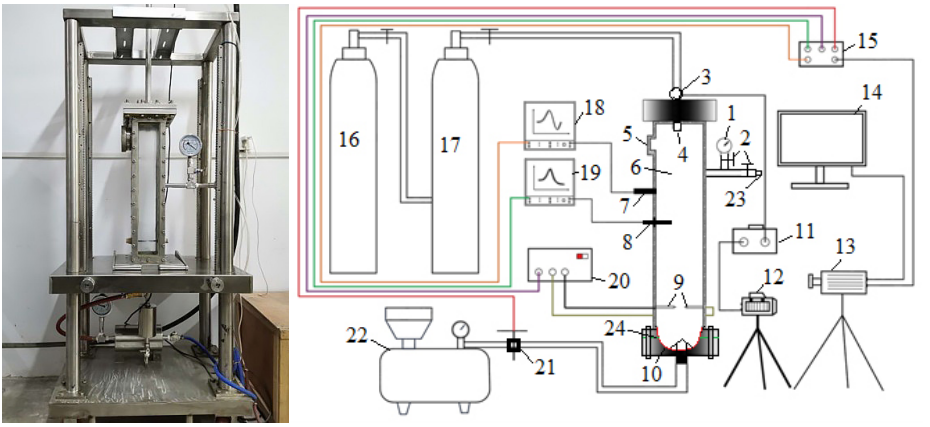

(a) (b)

Figure 2. Physical picture (a) and schematic diagram (b) of the suspended HMX explosion device: 1 – vacuum meter, 2 – ball valve, 3 – quick-opening device, 4 – centrifugal nozzle, 5 – bursting disc, 6 – explosion chamber, 7 – pressure transducer, 8 – thermocouple, 9 – electrode, 10 – dust nozzle, 11 – controller, 12 – flame detector, 13 – high-speed camera, 14 – computer, 15 – time controller, 16 – nitrogen tank, 17 – water tank, 18 – pressure measuring analyzer, 19 – temperature tester, 20 – ignition unit, 21 – solenoid valve, 22 – air compressor, 23 – "to vacuum pump", 24 – flange

The experimental process was as follows:

1) Before conducting the experiment, each module was connected as illustrated in Figure 2(b) and the control program was debugged to ensure that powder spraying, ignition, and data acquisition could be controlled automatically.
(2) The high-speed camera was fixed, adjusted for image clarity, and set to an acquisition frequency of 1000 frames per second (fps).
(3) Flange (24) was opened to separate the powder groove from the explosion chamber, and to evenly disperse the required mass of HMX dust around the dust nozzle. The electrode spacing was adjusted to 2-5 mm, and then connected to the flange.

(4) Vacuum in the explosion chamber was adjusted to the specified pressure, allowed to stand for 3 min, and then checked for airtightness. If the airtightness is satisfactory, proceed to the next step.
(5) The air compressor was turned to the specified pressure.
(6) Distilled water was injected into the water tank, the inlet valve opened, and the pressure-reducing valve of the nitrogen tank adjusted to achieve the required pressure for the experiment.
(7) The delay time for each module was set using a time controller and the experiments conducted.
(8) The data was saved, the gas source was turned off, the bottom flange was opened, the explosion chamber was cleaned and dried , and the next experiment was organised.

2.3 Combustion suppression of stacked HMX using water mist

The stacked HMX combustion suppression test device is illustrated in Figure 3. The experimental device comprised a sample combustion module, a water mist module, a timing controller, and a data acquisition module. The combustion module consisted of an ignition device and a combustion platform. The water mist module included a water tank, a nitrogen source, and a spraying device. The data acquisition system featured a high-speed camera and a computer.

(a)

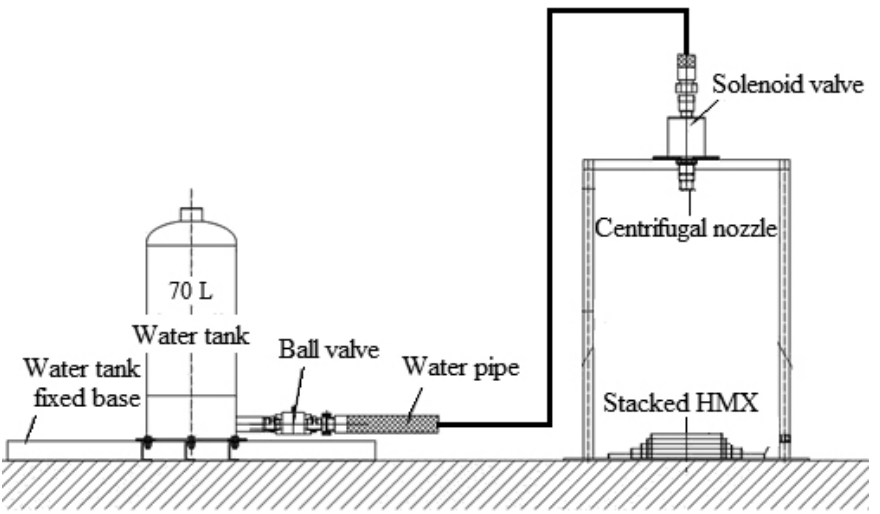

(b)

Figure 3. Physical picture (a) and schematic diagram (b) of the stacked HMX combustion device

The experimental process was outlined as follows:

(1) Before conducting the experiment, each module was connected as illustrated in Figure 3(b) and the control program was debugged to ensure that ignition and data acquisition can be controlled automatically.
(2) The high-speed camera was fixed and adjusted for image clarity, and the acquisition frequency was set to 1000 FPS for the experiment.
(3) HMX was placed on the combustion platform according to the specified dimensions.
(4) Distilled water was injected into the water tank, the inlet valve was opened, and the pressure-reducing valve of the nitrogen cylinder was adjusted to achieve the required pressure for the experiment.
(5) The delay time for each module was set using a time controller and the experiments were conducted.
(6) The data was saved, the gas source was turned off, the site was cleaned, and the next experiment was organised.

3 Inhibitory Effect of Water Mist on Suspension HMX Explosions

3.1 Explosion characteristics of suspension HMX explosions with different masses

Considering the actual concentration values of the HMX suspension generated during the production process and the pressure resistance limit of the square tube, five masses of HMX (1.5, 2.5, 3.5, 4.5, and 5.5 g) were selected for experimentation, corresponding to concentrations of 211.27, 352.11, 492.96, 633.80, and 774.65 $g \cdot m^{-3}$, respectively. The flame propagation, explosion pressure, and explosion temperature of the suspension HMX explosions at different concentrations were recorded to compare the explosion inhibition effects of water mist.

3.1.1 Flame propagation of suspended HMX with different masses

The propagation of flame from the explosion of suspended HMX with different masses in the square tube is illustrated in Figure 4. Taking a 4.5 g HMX dust explosion as an example, as illustrated in Figure 4(d), it was observed that when the HMX is ignited (at 0 ms), an irregular orange flame cluster forms within 10 ms. At approximately 11 ms, the flame front reaches the top of the square tube, and the flame appears bright white. Due to the constraints of the square tube, the flame does not continue to propagate once it reaches the top of the square tube, but becomes increasingly bright, peaking in intensity around 28 ms. Following this period of intense brightness, the flame gradually transitions to yellow and begins to dissipate from the center of the square tube.

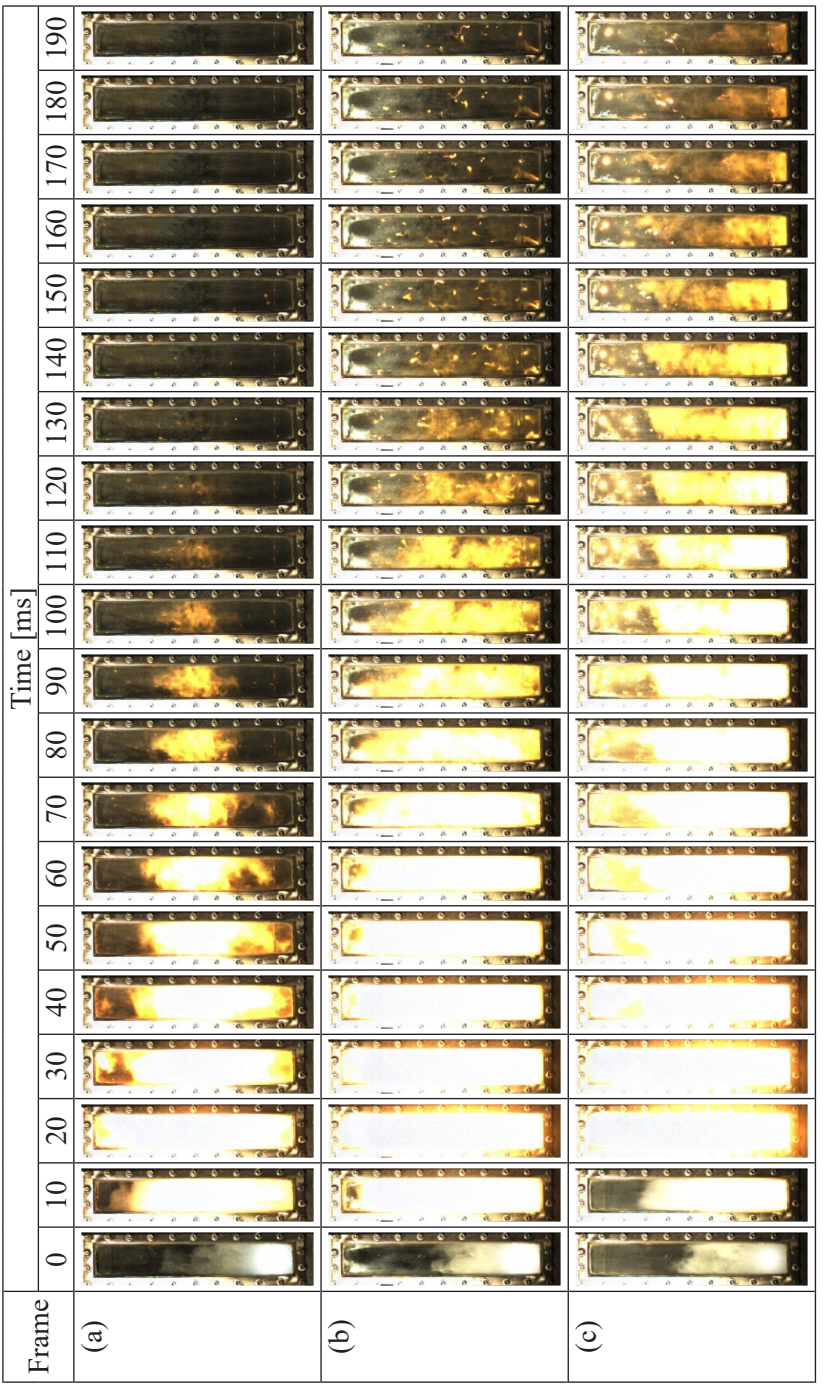

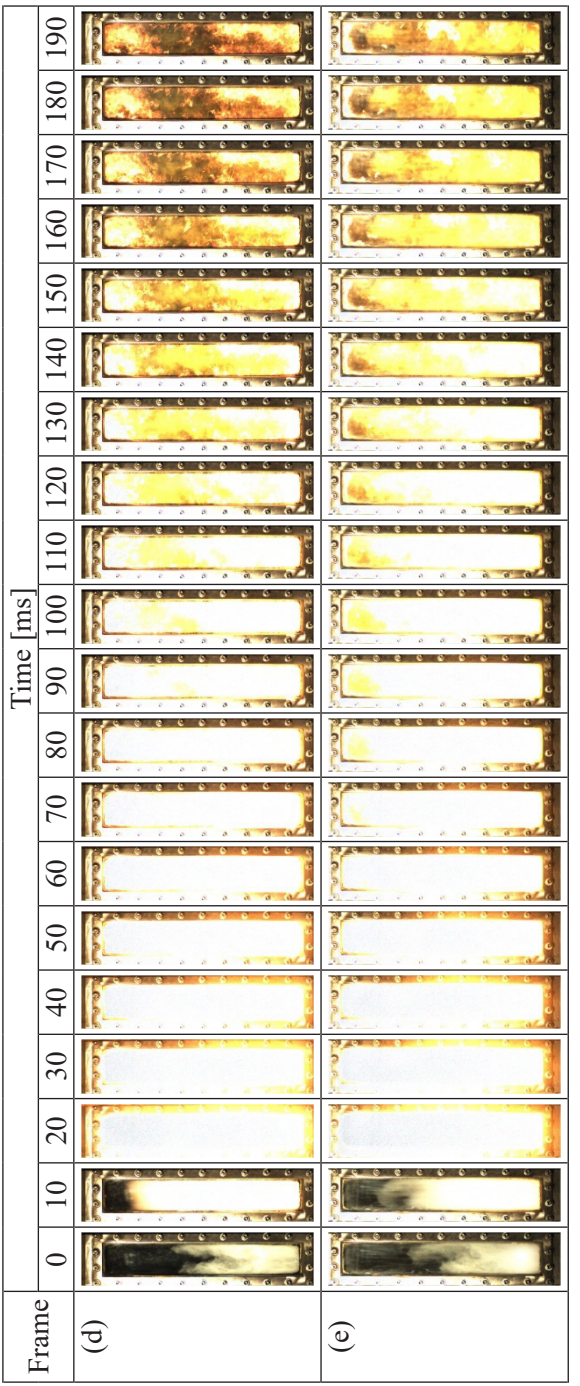

Figure 4. Flame propagation of HMX dust explosions with different masses of HMX: 1.5 (a), 2.5 (b), 3.5 (c), 4.5 (d) and 5.5 g (e)

During the growth stage of HMX combustion, a yellow flame zone is observed at the front of the white flame. This yellow zone indicates the stage at which HMX dust particles begin to ignite or are actively burning. The red zone at the leading edge of the flame front represents the pre-reaction phase between HMX dust and air, with its presence attributed to the thermal radiation emitted by the flame. As the propagation speed of the HMX flame changes, the thickness of the yellow flame zone also varies. When the HMX flame speed is low, the yellow flame zone is thicker; conversely, when the flame propagation speed is high, the yellow flame zone becomes thinner.

Comparing the flame propagation of 1.5 to 5.5 g of HMX dust in the square tube, it was evident that as the mass of HMX dust was increased, the maximum duration of the dust explosion's flame became longer, and the flame intensity increased. Additionally, the time from ignition to the conclusion of the HMX dust explosion was also extended.

3.1.2 Explosion pressure of suspended HMX with different masses

The explosion pressure of suspended HMX with different masses within the square tube is illustrated in Figure 5. From Figure 5(a), it is evident that following the explosion of the HMX dust with different masses in the square tube, two distinct peaks emerge within 250 ms. The pressure collection instrument was activated at 0 ms. At 20 ms, the solenoid valve opened, allowing for the aeration and spraying of the dust. The electrode discharged when the interior of the explosion chamber returned to atmospheric pressure at 80 ms. Within the 0-10 ms interval after ignition, the suspended HMX dust was ignited. Due to the limited quantity of HMX dust participating in the reaction during this initial period, the rate of pressure increase was minimal. However, 10 ms later, a large amount of suspended HMX dust was ignited, resulting in a marked increase in the rate of pressure rise. This led to the appearance of the first peak on the pressure curve. A negative pressure zone formed at the center of the explosion shortly after the explosion concluded, mixing the surrounding air with HMX dust, which triggered a second explosion and the formation of a second peak.

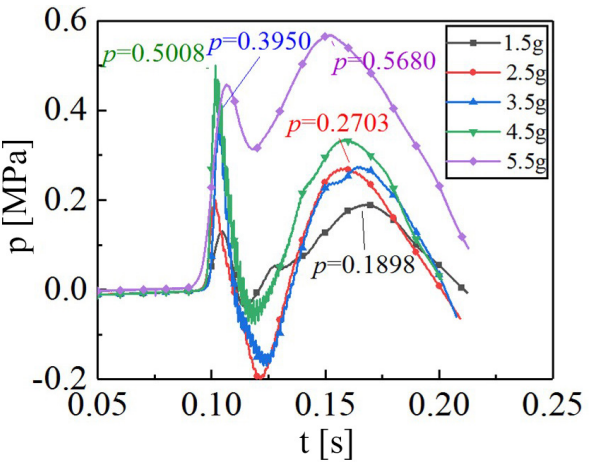

(a)

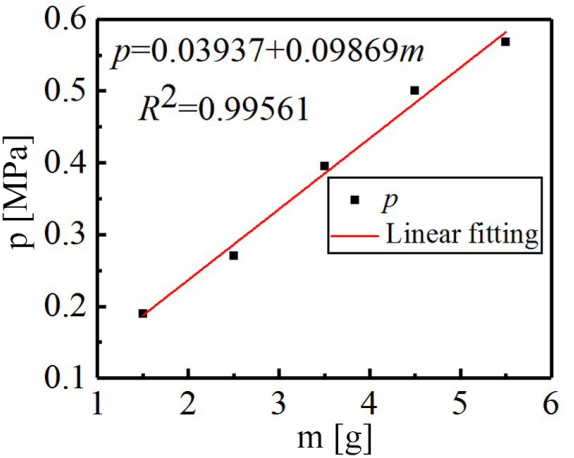

(b)

Figure 5. Explosion pressure of suspended HMX with different masses: pressure curve (a) and pressure values (b)

From Figure 5, it is evident that the maximum explosion pressures (p_{max}) from 1.5, 2.5, 3.5, 4.5, and 5.5 g of HMX dust are 0.1898, 0.2703, 0.3950, 0.5008, and 0.5680 MPa, respectively. As the mass is increased, the explosion pressure from the HMX dust exhibits a linear increase.

3.1.3 Explosion temperature of suspended HMX with different masses

The explosion temperatures of suspended HMX with different masses within the square tube are illustrated in Figure 6. From Figure 6, it can be observed that the maximum explosion temperatures (T_{max}) from 1.5, 2.5, 3.5, 4.5, and 5.5 g of HMX dust were 528, 591, 736, 840, and 915 °C, respectively. As the mass is increased, the explosion temperature from the HMX dust exhibits a linear increase.

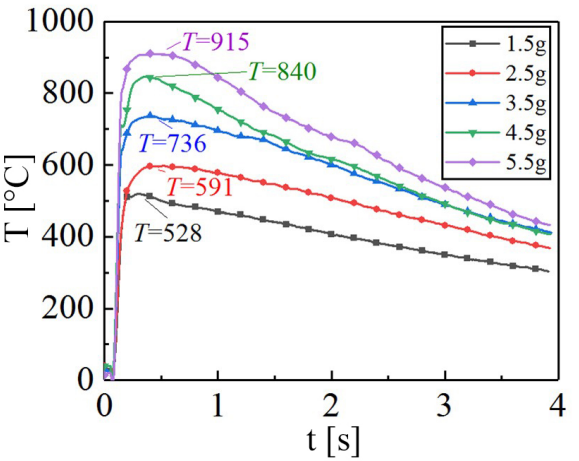

(a)

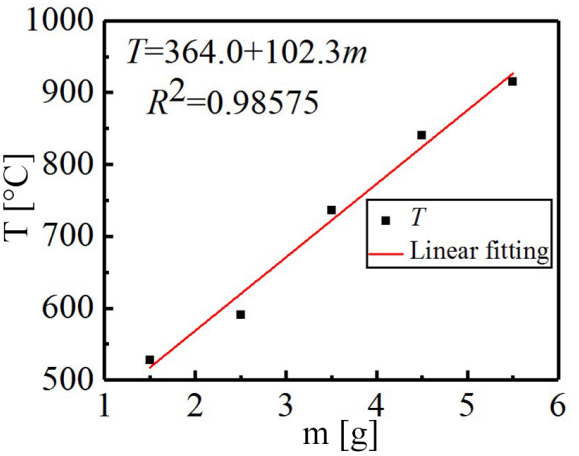

(b)

Figure 6. Temperature curve (a) and temperature values (b) of suspended HMX from different masses of HMX

Based on the data regarding flame propagation, explosion pressure, and temperature from HMX dust explosions from varying masses of HMX, significant differences were observed in these parameters when water mist was introduced compared to conditions without it. Taking these differences into account and prioritizing experimental safety, a mass of 4.5 g of HMX with a dust concentration of 633.80 $g \cdot m^{-3}$ was selected for testing the effectiveness of water mist in inhibiting explosion.

3.2 Inhibitory effect of water mist on HMX dust explosions

According to our previous research [29, 30], water mist sprayed by a centrifugal nozzle with an aperture of 2.4 mm demonstrated a superior suppression effect on explosive dust explosions. Consequently, we selected a centrifugal nozzle with an aperture of 2.4 mm to investigate the suppression effect of water mist on HMX dust explosions at an HMX concentration of 633.8 $g \cdot m^{-3}$.

3.2.1 Flame propagation of HMX dust explosions under varying spray pressures

The effect of water mist on the propagation of HMX flames at various spray pressures is illustrated in Figure 7. By comparing Figure 7 and Figure 4(d), it is evident that the addition of water mist during the propagation of the HMX dust explosion causes the upper flame in the square tube to become rapidly extinguished. However, the lower flame appeared to be discrete, with the flame at the edge exhibiting an orange-red colour. As the spray pressure was increased, the flux of the water mist also rose, resulting in a progressively shorter flame extinction time and an increasingly rapid extinction rate.

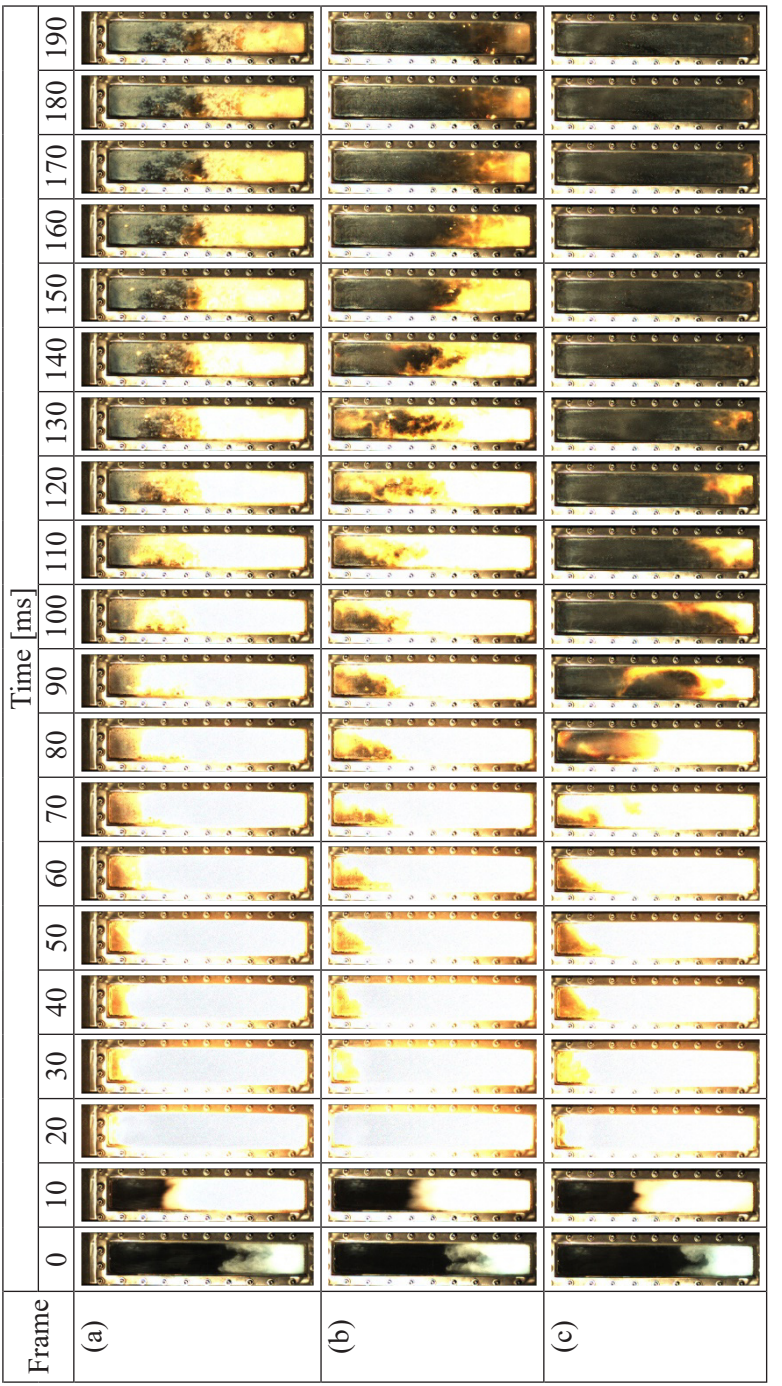

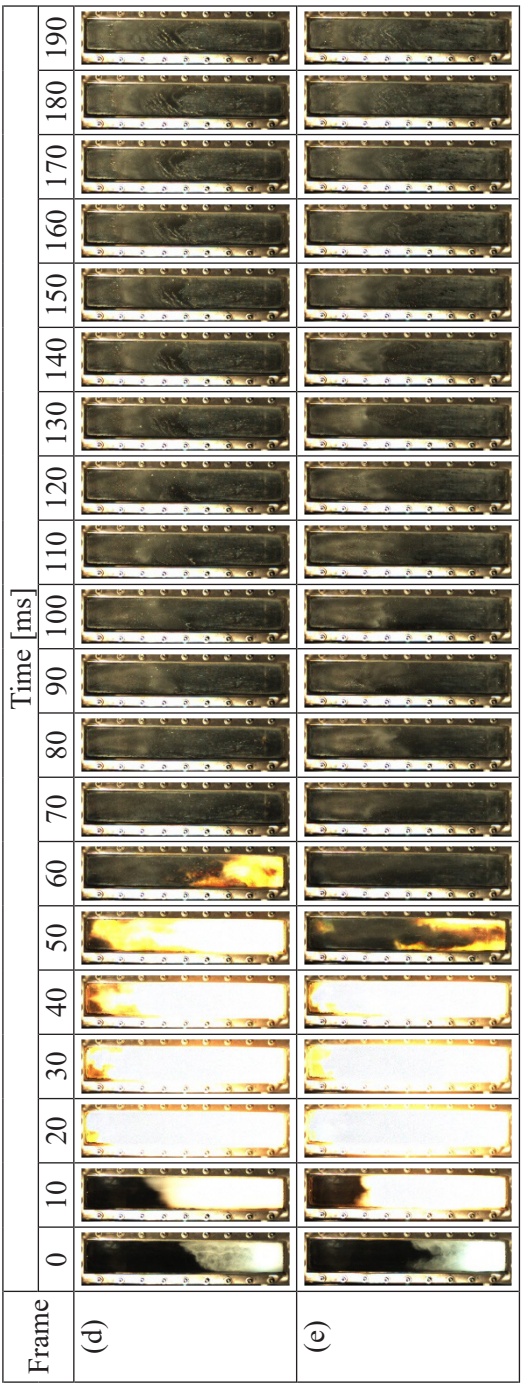

Figure 7. Flame propagation of an HMX dust explosion under different water spray pressures: 0.5 (a), 1 (b), 2 (c), 3 (d) and 4 MPa (e)

In summary, as long as water mist is present, it can hinder the flame propagation of HMX dust explosions. As the spray pressure was increased, the intensity of the combustion reaction was effectively reduced, the duration of flame combustion was shortened, and the suppression effect of the water mist on the flame propagation of HMX dust explosions could be enhanced.

3.2.2 Influence of different spray pressures on the explosion pressure of HMX dust

The pressure variations of the HMX dust explosion at different spray pressures are illustrated in Figure 8. As the spray pressure was increased from 0.5 to 4.0 MPa, the maximum explosion pressures (p_{max}) recorded were 0.4518, 0.3910, 0.3406, 0.2916, and 0.2402 MPa, respectively. The pressure peaks were reduced by 9.8%, 21.9%, 32.0%, 41.8%, and 52.0%, respectively, compared to a pressure of 0.5008 MPa observed without water mist. These experimental results indicate that as the spray pressure is increased, the measured p_{max} in the explosion chamber decreased. This suggests that the inhibitory effect of water mist on the explosion of HMX dust is significantly enhanced with higher spray pressures. Furthermore, as the spray pressure is increased, the rate of pressure rise decreased prior to reaching the initial peak pressure, and the time at which the initial peak occurs was delayed.

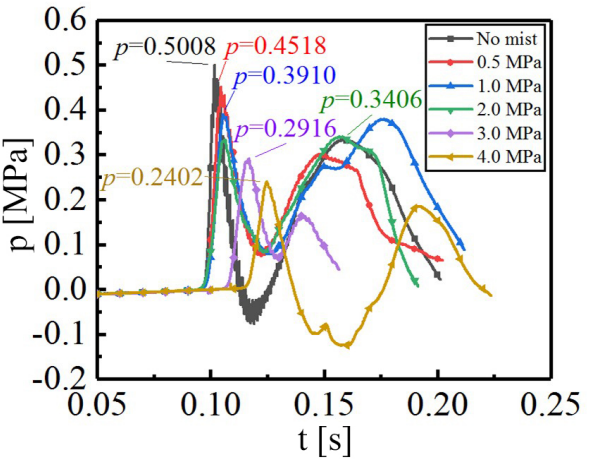

Figure 8. Pressure curves of HMX explosions under different water spray pressures

3.2.3 Influence of different spray pressures on the explosion temperature of HMX dust

The temperature variations of the HMX dust explosion at different spray pressures are illustrated in Figure 9. When the spray pressure was increased from 0.5 to 4.0 MPa, the maximum explosion temperatures (T_{max}) recorded were 670, 620, 462, 286, and 132 °C, respectively. These temperature peaks were reduced by 20.2%, 26.2%, 45.0%, 66.0%, and 84.3%, respectively, compared to the maximum temperature of 840 °C observed without water mist. These experimental results indicate that with the addition of water mist and an increase in spray pressure, the time at which the explosion temperature of HMX dust reached its maximum value was consistently delayed. Furthermore, after reaching this maximum value, the explosion temperature decreased rapidly. This demonstrated that as the spray pressure was increased, water mist can effectively lower the temperature in the reaction space and preheating zone.

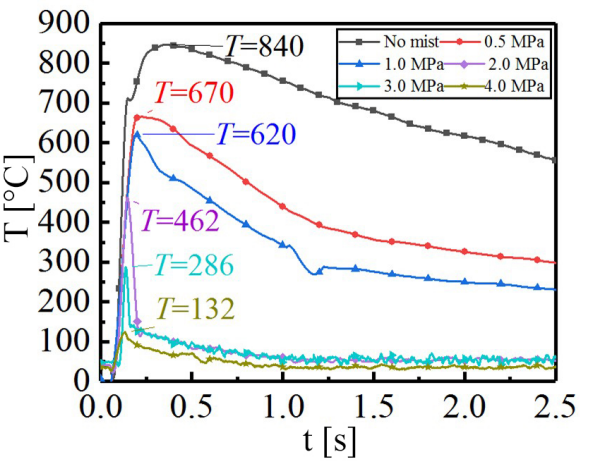

Figure 9. Temperature curves of HMX explosions under different water spray pressures

4 Inhibitory Effect of Water Mist on Stacked HMX Combustions

As in our previous research [30], the mass of HMX used in the experiment was 200 g, and the dimensions of the stack were Φ12×3 cm.

4.1 Combustion characteristics of stacked HMX without water mist

A high-speed camera was positioned 5 m away from the center of the stacked HMX during the experiment. A resistance wire was utilized to ignite the HMX, which was inserted approximately 1 cm below the surface. The combustion flame from the HMX is shown in Figure 10.

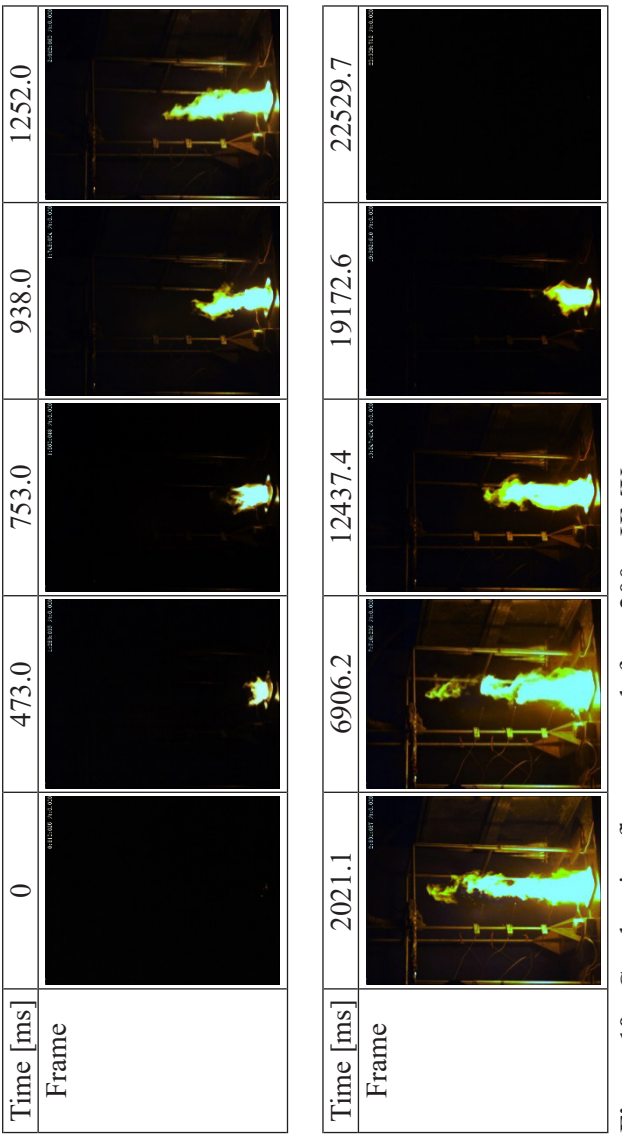

Figure 10. Combustion flame growth from 200 g HMX

The ignition time was recorded as 0 ms. At 473.0 ms after ignition, the flame height had risen to approximately 15 cm. After 753.0 ms, the flame front had reached the first thermocouple position, at a height of approximately 25 cm. Both the brightness and height of the flame had increased. At 938.0 ms after ignition, the flame height had reached the second thermocouple position, which was at about 50 cm. The lower part of the flame was bright white, emitting a dazzling light. The flame took on the shape of a long cylinder, with the upper part displaying an orange-yellow colour and scattered flames. At 1252.0 ms after ignition, the combustion flame had reached the third thermocouple position, which was at about 70 cm. At 2021.1 ms after ignition, the dispersion at the top of the flame intensified, and the instantaneous maximum height of the flame reached the nozzle height of approximately 100 cm. Subsequently, the flame fluctuated within this height range and persisted for 6906.2 ms. HMX then entered a phase of combustion attenuation until it became extinguished at 22529.7 ms. The total duration of the combustion process was approximately 22.53 s.

4.2 Combustion characteristics of stacked HMX with water mist

Referring to our previous research [30, 31], a half-inch centrifugal nozzle was selected for the combustion extinguishment study of stacked HMX. The interaction between the HMX flame and the water mist under spray pressures of 0.5, 1, 2, 3, and 4 MPa is illustrated in Figure 11. The experimental data are presented in Table 1.

Table 1. Suppression data for 200 g HMX combustion with water mist (nozzle distance 1 m)

Spray pressure [MPa]	Moment of water mist action [ms]	Moment of flame extinction [ms]	Fire extinguishing time [ms]
0.5	7851.24	8136.25	285.01
1.0	7936.24	8165.25	229.01
2.0	8000.24	8164.25	164.01
3.0	7968.24	8066.25	98.01
4.0	7841.24	7890.24	49.00

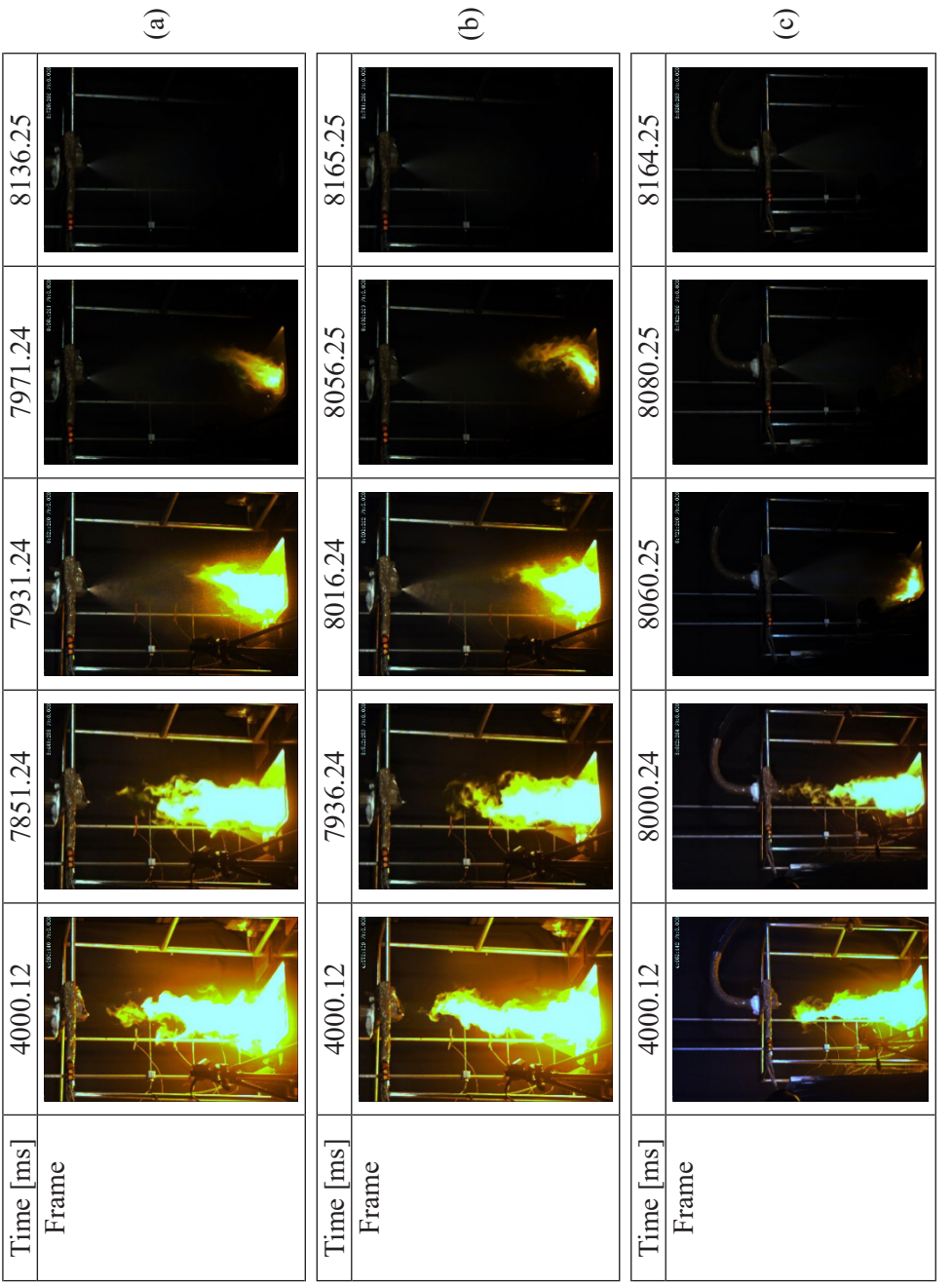

Time [ms]	4000.12	7968.24	8018.24	8048.25	8066.25
Frame		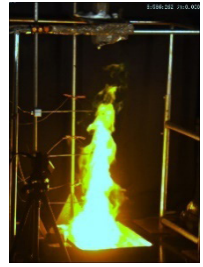			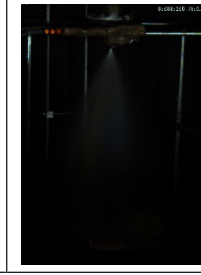

(d)

Time [ms]	4000.12	7841.24	7881.24	7886.24	7890.24
Frame		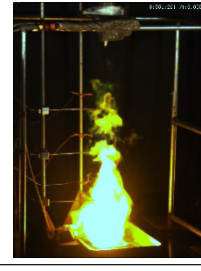	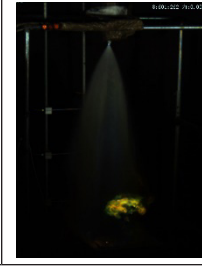	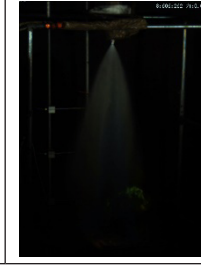	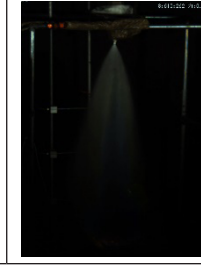

(e)

Figure 11. Combustion flame growth for 200 g HMX with water mist under different water spray pressures: 0.5 (a), 1 (b), 2 (c), 3 (d) and 4 MPa (e)

It can be observed from Table 1 and Figure 11 that the extinction times of the HMX combustion flame are 285.01, 229.01, 164.01, 98.01, and 49.00 ms, respectively, under water mist with spray pressures of 0.5, 1, 2, 3, and 4 MPa. The extinguishing time of the HMX combustion flame decreased as the spray pressure was increased.

Taking the fire extinguishing test with a spray pressure of 3.0 MPa as an example, the instantaneous maximum height of the flame reached 1.0 m approximately 4000.12 ms after ignition. The water mist was activated at 7968.24 ms. By 8018.24 ms, just 50 ms after the water mist was initiated, the flame had been significantly suppressed due to the water mist. However, the lower portion of the flame remained quite bright. Approximately 80 ms after the water mist was activated, the flame was almost extinguished. At 8066.25 ms, which was 98.001 ms after the water mist was turned on, the flame was completely extinguished.

The process of fire extinguishment can be divided into three stages. Firstly, when the water mist comes into contact with the combustion flame from stacked HMX, the flame is initially suppressed by the water mist, although it may briefly intensify. Secondly, as more water mist enters the combustion flame plume, it absorbs a large amount of heat, lowering the temperature of the combustion zone and reducing the resistance of the water mist as it moves towards the combustion area. The flame is gradually enveloped by the water mist, which pushes it closer to the surface of the stacked HMX. Finally, the water mist penetrates the flame zone and reaches the surface of the stacked HMX, continuously reducing the combustion temperature and minimizing the evaporation of combustible gases, ultimately leading to the extinguishment of the flame.

5 Mechanisms of Water Mist Inhibition on HMX Dust Combustions and Explosions

5.1 Energy absorption during the evaporation of water mist droplets

The energy absorption during the evaporation of droplets is crucial for suppressing explosions. To quantitatively evaluate the evaporation time, the evaporation behaviour of droplets was examined without considering the effects of coupled flow [32], as follows:

$$t_v = \frac{d^2\rho}{8\Gamma_v \ln(1+\frac{m_{v,0}-m_{v,\infty}}{1-m_{v,0}})} \quad (1)$$

where t_v represents the evaporation time (in s), d denotes the initial diameter of the droplet (in m), ρ is the density of liquid water, with a value of $\rho = 1000$ kg·m^{-3}, Γ_v is the water vapour exchange coefficient, given as $\Gamma_v = 2.6\times10^{-5}$ kg·ms^{-1}, $m_{v,0}$ indicates the mass fraction of water vapour in the mixture at temperature T (in K) at the droplet surface and $m_{v,\infty}$ represents the mass fraction of water vapour away from the surface at temperature T (in K).

The variation in droplet vaporization time as a function of droplet size, ranging from 1 to 1000 μm, is illustrated in Figure 12. It is important to note that the vaporization times for nearly micron-sized droplets begin in the microsecond range and extend to seconds for larger droplets measuring 1000 μm. At the elevated temperatures encountered in shock fronts, it is anticipated that these time scales will be significantly shorter. However, due to the extremely high velocities involved, the residence time will be very brief. Consequently, only droplets with vaporization time scales of microseconds or less will effectively respond to shock energy extraction. Additionally, droplets in fine mist form will demonstrate vaporization time scales of microseconds or less at these temperatures.

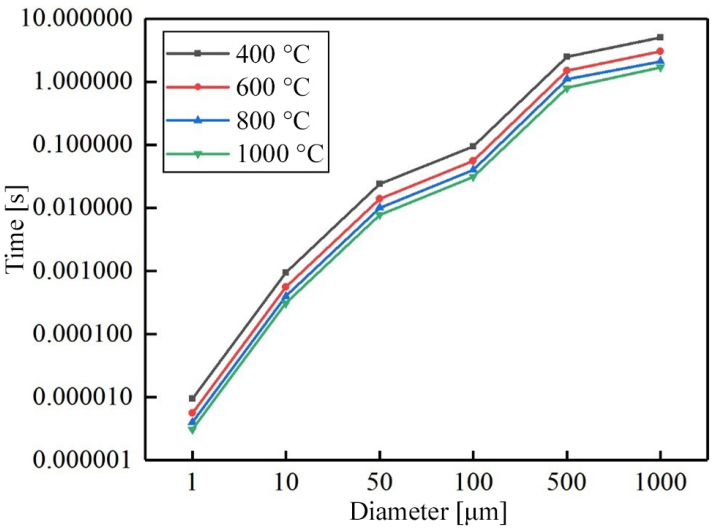

Figure 12. Evaporation time scales of droplets from the shock-induced droplet breakup process

5.2 Heat radiation block of water mist droplets

The effective transfer of thermal radiation is a crucial factor in sustaining combustion reactions. Water mist can significantly obstruct the thermal radiation produced during combustion. Log [33] modelled the flame as a black body radiating at a uniform temperature and investigated the impact of water mist on radiation absorption. The study revealed that the thermal radiation transmission rate was 28% when the incident thermal radiation passed through a water mist with D_{10}=50 μm and D_{90}=100 μm. The thermal radiation attenuation rate (η) due to the presence of water mist can be calculated using Equation 2.

$$\eta = 1 - \frac{\int_0^\infty E_{\lambda,T}\gamma_\lambda \mathrm{d}\lambda}{\int_0^\infty E_{\lambda,T}\mathrm{d}\lambda} \tag{2}$$

where $E_{\lambda,T}$ is the radiation force of the flame (in $Wm^{-2}\cdot m^{-1}$), γ_λ is the transmittance of the flame spectra through a specific width of a water mist area and λ is the wavelength of radiation (in m). Under conditions of constant water mist particle size, the attenuation rate of thermal radiation significantly improves as the mist flux increases.

5.3 Hot surface infiltration of water mist droplets

In addition to absorbing the heat generated by the reaction, some of the water mist in the explosion reaction zone can also absorb heat and cool by infiltrating the surfaces of both burned and unburned reactants. When droplets pass through the shock wave front, penetrate the flame zone, and reach the surfaces of the reactants, they can effectively absorb the surface heat, thereby slowing the heat transfer rate on the reactants' surfaces and weakening the further propagation of the flame.

5.4 Chemical inhibition of water mist droplets

Water molecules are suspended in the explosion reaction zone, and free radicals such as H· and OH· generated by water molecules can participate in the explosion chain reaction, thereby reducing the rate of explosion chemical reactions [34]. Some of the free radicals produced during the chain reaction process are neutralized through collisions with droplets, which decreases the number of free radicals available for the chain reaction and further accelerates the extinguishing of flames.

6 Conclusions

The inhibitory effect of water mist with different spray pressures on HMX explosions and combustions was investigated. The primary conclusions are as follows:

- As the concentration of suspended HMX is increased, both the duration of the HMX dust explosion flame and its brightness are also increased. Furthermore, the explosion pressure and temperature rise in a nearly linear fashion.
- The inhibitory effect of water mist on suspended HMX explosions is enhanced with increasing spray pressure. When the spray pressure was increased from 0.5 to 4.0 MPa, the pressure peaks were reduced by 9.8%, 21.9%, 32.0%, 41.8%, and 52.0%, respectively, compared to a pressure of 0.5008 MPa without water mist. The temperature peaks were reduced by 20.2%, 26.2%, 45.0%, 66.0%, and 84.3%, respectively, compared to a temperature of 840 °C without water mist.
- The extinguishing time of stacked HMX combustion is decreased as the water spray pressure is increased. At a spray pressure of 4.0 MPa, the extinguishing time for stacked HMX combustion is only 49.00 ms.

Acknowledgments

This work was supported by the National Natural Science Foundation of China (No. 52276138) and the Fundamental Research Program of Shanxi Province (No. 202203021212160).

References

[1] Braidech, M.M.; Neale, J.A.; Matson, A.F. *The Mechanisms of Extinguishment of Fire by Finely Divided Water.* New York: Underwriters' Laboratories Inc., **1955**.
[2] Rasbash, D.J.; Rogowshi, Z.W. Extinction of Fires in Liquids by Cooling with Water Sprays. *Combust. Flame* **1957**, *1*(4): 453-466.
[3] Wighus, R.; Aune, P.; Drangsholt, G. Full Scale Water Mist Experiments. *Proc. Int. Conf. Water Mist Fire Suppression Systems*, Sweden, **1993**.
[4] Wighus, R. Engineering Relations for Water Mist Fire Suppression Systems. *Proc. Halon Alternatives Technical Working Conf.,* **1995**.
[5] Mawhinney, J.R. Water Mist Fire Suppression Systems: Applications, Principles, and Limitations. *Int. Conf. Fire Protection in the HVDC Industry*, Vancouver, Canada, **1995**.
[6] Mawhinney, J.R.; Dlugogorski, B.Z.; Kim, A.K. A Closer Look at the Fire

Extinguishing Properties of Water Mist. *Proc. 4th Int. Assoc. Fire Safety Sci.,* **1994**.
[7] Han, Z.; Zhang, Y.; Du, Z.; Xu, F.; Li, S.; Zhang, J. New-type Gel Dry-Water Extinguishants and Its Effectiveness. *J. Cleaner Prod.* **2017**, *166*: 590-600; https://doi.org/10.1016/j.jclepro.2017.08.005.
[8] Lu, Z.; Gao, W.; Jiang, H.; Jin, S.; Nie, Z.; Zhao, F. Vented Flame Quenching Mechanism and Overpressure Prediction Model in Aluminum Dust Explosions. *Int. J. Therm. Sci*. **2025**, *210* paper 109623; https://doi.org/10.1016/j.ijthermalsci.2024.109623.
[9] Li, G.; Gao, W.; Jiang, H.; Liu, J.; Zhao, F.; Jin S.; Lu, Z. Ignition and Combustion of AlH_3-Nanoparticles: A Molecular Dynamics study. *Combust. Flame* **2024**, 269 paper *113667*; https://doi.org/10.1016/j.combustflame.2024.113667.
[10] Eriksson, S. *Water in Explosive Storage.* FortF/F Report C 104, Stockholm, **1974**.
[11] Keenan, W.A.; Wager, P.C. Mitigation of Confined Explosion Effects by Placing Water in Proximity of Explosives. *Proc. 25th Department of Defense Explosives Safety Semin.*, Anaheim, California, **1992**.
[12] Marchand, K.; Oswald, C.; Polcyn, M. Testing and Analysis Done in Support of the Development of a Container for On-Site Weapon Demilitarization. *Proc. 27th Department of Defense Explosives Safety Semin.*, Las Vegas, US-NV, **1996**.
[13] Schwer, D.; Kailasanath, K. *Blast Mitigation by Water Mist (1) Simulation of Confined Blast Waves*. Naval Research Laboratory, NRL/MR/6410-02-8636, **2002**.
[14] Schwer, D.A.; Kailasanath, K. Numerical Simulations of the Mitigation of Unconfined Explosions Using Water-mist. *Proc. Combust. Inst.* **2007**, *31*(2): 2361-2369; https://doi.org/10.1016/j.proci.2006.07.145.
[15] Resnyansky, A.D.; Delaney, T.G. *Experimental Study of Blast Mitigation in a Water Mist.* Defence Science and Technology Organisation, DSTO-TR-1944, 2006.
[16] Willauer, H.D.; Ananth, R.; Williams, F.W. *Blast Mitigation Using Water Mist: Test Series II.* Naval Research Laboratory, NRL/MR/6180-09-9182, **2009**.
[17] Ananth, R.; Willauer, H.D.; Farley, J.; Wiliamson, F.W. Effects of Fine Water Mist on a Confined Blast. *Fire Technol.* **2012**, *48*(3): 641-675; https://doi.org/10.1007/s10694-010-0156-y.
[18] Jiba, Z.; Sono, T.J.; Mostert, F.J. Implications of Fine Water Mist Environment on the Post-Detonation Processes of a PE4 Explosive Charge in a Semi-Confined Blast Chamber. *Def. Technol.* **2018**, *14*(5): 366-372; https://doi.org/10.1016/j.dt.2018.05.005.
[19] Zhao, H. Water Effects on Shock Wave Delay in Free Fields. *Explos. Shock Waves* **2001**, *21*(1): 26-28; https://scispace.com/papers/water-effects-on-shock-wave-delay-in-free-fields-2jl24gvleh.
[20] Zhao, H. Water Mitigation Effects on Explosion in Confined Chambers. *Explos. Shock Waves* **2002**, *22*(3): 252-256; https://scispace.com/papers/water-mitigation-effects-on-explosions-in-confined-chambers-32ohvkm3hn.
[21] Chen, L.; Zhang, L.; Fang, Q.; Mao, Y. Performance Based Investigation on the Construction of Anti-Blast Water Wall. *Int. J. Impact Eng.* **2015**, *81*: 17-33; https://doi.org/10.1016/j.ijimpeng.2015.03.003.

[22] Zhang, L.; Chen, L.; Fang, Q.; Zhang, Y. Mitigation of Blast Loadings on Structures by An Anti-Blast Plastic Water Wall. *J. Cent. South Univ.* **2016**, *23*(2): 461-469; https://doi.org/10.1007/s11771-016-3091-3.
[23] Xu, H.; Wang, Z.; Hu, H.; Sun, Z.; Shi, G.; Yang, J.; Shen, Z. Experimental Study of Air-gap Effect on Water Mitigation of Confined Explosion. *Acta Armamentarii* **2016**, *37*(8): 1443-1448; https://doi.org/10.3969/j.issn.1000-1093.2016.08.015.
[24] Xu, H.; Zhong, F.; Yang, J.; Zhang, D.. Experimental Study for Effects of Water and Its Container on Explosion Loading Near Explosive. *Explos. Shock Waves* **2016**, *36*(4): 525-531; https://doi.org/10.11883/1001-1455(2016)04-0525-07.
[25] Xu, H. *Mechanism and Effect of Water Mitigation on Confined Explosion Loading*. University of Science and Technology of China, Hefei, **2020**.
[26] Xu, H.; Cheng, L.; Zhang, D.; Zhang, F.; Shen, Z.; Liu, W.; Huang, S. Mitigation Effects on the Reflected Overpressure of Blast Shock with Water Surrounding An Explosive in a Confined Space. *Def. Technol.* **2021**, *17*(3): 1071-1080; https://doi.org/10.1016/j.dt.2020.06.026.
[27] Li, Y.; Ren, G.; Zhang, W. Water Mitigation Effect Under Internal Blast. *Explos. Shock Waves* **2017**, *37*(6): 1080-1086.
[28] Chen, P.; Hou, H.; Liu, G.; Zhu, X.; Zhang, G. Experimental Investigation on Mitigating Effect of Water Mist on the Explosive Shock Wave Inside Cabin. (in Chinese) *Acta Armamentarii* **2018**, *39*(5): 927-933; https://doi.org/10.3969/j.issn.1000-1093.2018.05.012.
[29] Hu, L.; Liu, Y.; Yang, Y. Inhibition Effect of Water Mist on RDX Dust Explosion. *Explos. Shock Waves* **2024**, *44*(5): 055401.
[30] Liu, Y. *Explosion Suppression of Suspended and Stacked Explosives and Propellants by Water Mist.* North University of China, Taiyuan, **2021**.
[31] Wei, X.; Hu, S.; Dong, G.; Hu, L.; Cui, C.; Feng, Y.; Yao, Y. Research on Combustion Inhibition of Water Mist on PBXN-5. *Explos. Mater.* **2021**, *50*(6): 14-20; https://doi.org/10.3969/j.issn.1001-8352.2021.06.003.
[32] Adiga, K.C.; Willauer, H.D.; Ananth, R.; Williams, F.W. Implications of Droplet Breakup and Formation of Ultra Fine Mist in Blast Mitigation. *Fire Safety J.* **2009**, *44*(3): 363-369; https://doi.org/10.1016/j.firesaf.2008.08.003.
[33] Log, T. Radiant Heat Attenuation in Fine Water Sprays. *Proc. Int. Fire Sci. Eng. Conf.*, Cambridge, UK, **1996**.
[34] Holborn, P.G.; Battersby, P.; Ingram, J.M.; Averill, A.F.; Nolan, P.F. Modelling the Mitigation of Hydrogen Deflagrations in a Vented Cylindrical Rig with Water Fog and Nitrogen Dilution. *Int. J. Hydrogen Energy* **2013**, *38*(8): 3471-3487; https://doi.org/10.1016/j.ijhydene.2012.12.134.

Contribution

Yang Liu: conception, foundations, performing the experimental part
Yu Qiu: methods
Huinan Wang: performing the experimental part

Keqin Zhang: methods
Bowen Du: performing the experimental part
Yuewen Lu: performing the experimental part
Jianren Zhang: performing the statistical analysis
Lei Sun: performing the experimental part
Zhixing Lv: methods
Lishuang Hu: conception, foundations, performing the statistical analysis

Submitted: October 26, 2024
Revised: March 24, 2025
First published online: March 31, 2025